IC/87/416

INTERNATIONAL CENTRE FOR THEORETICAL PHYSICS

INTERFERENCE EFFECTS IN THE NONLINEAR CHARGE DENSITY WAVE DYNAMICS

D. Jelčić

A. Bjeliš

and

I. Batistić

INTERNATIONAL ATOMIC ENERGY AGENCY

UNITED NATIONS EDUCATIONAL, SCIENTIFIC AND CULTURAL ORGANIZATION

IC/87/416

International Atomic Energy Agency
and
United Nations Educational Scientific and Cultural Organization
INTERNATIONAL CENTRE FOR THEORETICAL PHYSICS

INTERFERENCE EFFECTS IN THE NONLINEAR CHARGE DENSITY WAVE DYNAMICS *

D. Jelčić
Department of Physics, Faculty of Sciences, University of Zagreb,
P.O.B. 162, 41001 Zagreb, Yugoslavia,

A. Bjelis **
International Centre for Theoretical Physics, Trieste, Italy

and

I. Batistić
Institute of Physics of the University of Zagreb,
P.O.B. 304, 41001 Zagreb, Yugoslavia.

MIRAMARE - TRIESTE
December 1987

* Submitted for publication.

** Permanent address: Institute of Physics of the University of Zagreb,
P.O.B. 304, 41001 Zagreb, Yugoslavia.

ABSTRACT

The main features of the nonlinear charge density wave transport in the external dc-ac field are shown to be the natural consequences of resonant phase slip diffusion. This process is treated numerically within the time dependent Landau-Ginzburg model, developed by Gor'kov. The resonances in the ac field are manifested as Shapiro steps in I-V characteristics, present at all rational ratios of internal frequency of current oscillations and external ac frequency. The origin of Shapiro steps, as well as their form and heights, are considered in detail. In particular, it is shown that close to resonances the phase slip voltage acquires a highly nonsinusoidal modulation which leads to the appearance of low frequency and satellite peaks in the Fourier spectrum. Taking into account the interference of adjacent phase slips and the segment or domain structure of physical samples, we interpret the finite width of steps, side wings, synchronization, incomplete and complete mode locking and some other effects observed in numerous experiments on $NbSe_3$ and other CDW materials.

1. INTRODUCTION

In the last decade an extra nonlinear conductivity above a finite treshold electric field is observed in various highly anisotropic materials which undergo the Peierls transition[1]. This onset of the collective transport due to the moving charge density wave (CDW) is often accompanied by the multiharmonic voltage oscillations, so called narrow band noise (NBN), with a frequency proportional to the excess CDW current. The phenomenon closely related to the NBN are Shapiro steps, appearing in dc current-voltage curves when an additional external ac current is applied in the regime of a nonlinear transport. These steps were noticed[2,3] at many commensurate ratios of the external frequency and the fundamental frequency of the NBN. They are usually interpreted as the interference effects, due to which the CDW velocity (i.e. current) is mode locked onto the external ac drive. The mechanism responsible for the NBN and Shapiro steps is however still a matter of numerous experimental and theoretical investigations. We continue by emphasizing some questions related to this problem.

The usual understanding of the onset of collective CDW transport is based on the model of interaction of the CDW with impurities which are randomly distributed within the bulk of the specimen[4,5]. Impurities introduce a finite potential barrier for the CDW motion and break the translational invariance of the system. In the crudest approximation the translational invariance is restored by replacing the impurity potential by an effective space independent "bulk" potential which depends only on the overall CDW phase[6,7]. Although conceptually

questionable for an infinite system in which the averaging over impurities would lead to the vanishing mean potential[8], this approach of rigid CDW accounts for the CDW depinning at finite electric fields and the appearance of the coherent current oscillations. Finite and smooth spatial variations of the impurity potential lead to finite Lee-Rice correlation length for phase fluctuations and give a more elaborate description of the bulk CDW depinning and of the CDW elasticity[8], characterized by the phason mode with a finite long-wavelength gap[9]. However, no coherent oscillations follow from the motion of deformable CDW in the random potential[8]. This completes the main conclusions of the perturbative "bulk" description of CDW dynamics.

A qualitatively different situation is realized when the specimen contains very strong defects which are of finite extension and introduce local potentials presumably much higher than the bulk pinning potential. Such a defect acts as an obstacle, i.e. as an effective boundary condition for the CDW motion. For the electric field exceeding the treshold field for the "bulk" depinning, the CDW will start to slide, but will adjust locally its velocity, as well as its phase and amplitude, in order to accommodate these "boundary conditions". At such places the CDW velocity is expected to be extremely low, leading to large local deformations of the CDW phase. The resulting strains in the CDW can eventually provide an amount of energy sufficient to overcome locally the condensation energy and to relax the CDW amplitude, at least through a process of its temporal variations.

The way in which obstacles affect the local CDW ordering depends also on their transverse dimensions. For an obstacle of small

transverse size $d_\perp$ ($d_\perp < \xi_\perp$, where $\xi_\perp$ is the transverse correlation length), a kind of "hydrodynamical" flow around it could be expected. The detailed analysis of such CDW motion is in progress. The obstacles which are transversally extended enough ($d_\perp \geq \xi_\perp$) present, on contrary, barriers which can prevent locally the CDW translation. In order to maintain the continuity of the total current through the specimen, a CDW current has to convert to the ohmic one. This conversion is proposed[10] to be performed through the succession of the phase slippages (PS) in front of the barrier. The PS is the fast localized collapse of the CDW amplitude, and is an example of amplitude relaxation mentioned above. During one PS the CDW phase slips for one wavelength, i.e. for 2π. The periodic succession of PS's generates pulses in the voltage, which were interpreted as a source of NBN in CDW systems[10,11].

An accurate description of the CDW depinning, as well as of its dynamics above the treshold, should involve simultaneously both the "bulk" and the "local" mechanisms considered above. However, due to the complexity of such an approach, the usual starting points rely on the assumption that one of the mechanisms dominates in real systems and in a particular regime of fields ($E = E_t$ or $E \gg E_t$). It is widely accepted that the bulk mechanism (i.e. impurities) is responsible for the CDW depinning, especially in trihalcogenide materials, providing that the sample dimensions are large enough, and strong defects are very far one from another. Still, there are indications, e.g. from recent measurements on $NbSe_3$[12] and blue bronzes[13], that the circumference and, in some special circumstances, the electrical contacts and sample edges, regulate the CDW depinning even in

macroscopically large samples.

The regions of electrical contacts as the origin of NBN were first invoked in measurements of Ong and Verma[14]. These data initiated the theoretical studies[15,16] of the behaviour of CDW in a vicinity of such barriers at which the complete conversion from the collective to the ohmic conduction occurs. Many latter experiments were designed to locate the parts of the specimen in which NBN occurs. While some of them[15,16] confirmed the conclusions of Ref.[14], others showed[17,3] that the whole sample may participate in NBN production, i.e. that the sample interior cannot be excluded as the source of NBN. The further refinements of a mechanism responsible for NBN, if it is unique at all, are necessary for understanding of these findings. Regarding the approach which invokes the strong variations of CDW amplitude, it should be stressed that, beside contacts, the obstacles which affect CDW on the transverse scale larger than $\xi_\perp$ are perhaps often present even in the interior of samples. An indication for their presence is the switching in well defined localized segments of some $NbSe_3$ specimens[18].

The aim of the present work is to interpret Shapiro steps as the interference between the external ac field and the local generation of NBN through the PS process. We start from the Gor'kov's microscopic model[10], which leads to the nonlinear dynamical equations allowing for both phase and amplitude variations in the CDW. The numerical analysis[11] of these equations gave the detailed description of the generation of the PS's and the corresponding pulses in the voltage in presence of an external dc electric field.

The effects of a finite ac field within this model were until now

discussed[19] only in the limit of unphysically large electric fields in which an approximate analytical treatment is feasible. The partial suppression of nonlinearity in this limit gives resonances only at harmonic values of the external frequency. This analysis is here extended numerically to weaker electric fields, i.e. to the regime in which the NBN itself is highly multiharmonic[11]. We obtain the V(E) dependence with steps at both harmonic and subharmonic resonant ratios. The step heights follow the oscillatory dependence on ac amplitude, in agreement with experimental results[2,3]. We also analyze the modulations of the voltage in the vicinity of the resonances and show that a mismatch between the internal (ω_{int}) and field (ω_{ext}) oscillations results in rather sharp beats. The corresponding Fourier spectrum of the voltage contains satellites close to main resonant lines and an additional structure in the low frequency range, at $\omega \sim |\omega_{ext}-n\omega_{int}/m|$. Furthermore, the resonant behaviour is shown to depend significantly on a distance between the neighbouring barriers. For short enough distances, the PS's from two barriers interfere. This leads to a complete locking of the PS oscillations onto the external frequency and phase in a resonance band of finite width, which increases as the separation between the barriers decreases. Some of these results are preliminary reported in Ref.[20].

The article is organized as follows. In Section 2. we review shortly the Gor'kov's model, outline the main characteristics of the PS process in presence of dc fields and introduce the approximations relevant for numerical calculations. The numerical results for the CDW motion in the time dependent electric field are presented in Section 3. Particularly, the case of semi-infinite segments is analyzed in Section

3.1, while the effects of finite distance between the adjacent obstacles are considered in Section 3.2. In Section 4. we discuss our results and make a comparison with the actual experimental findings. Section 5. contains some concluding remarks.

2. MODEL

The effects of strong obstacles like contacts, strong lattice distortions, segment boundaries etc., are considered in Gor'kov's model separately from incoherent scatterings on randomly distributed weak defects (e.g. impurities). Close to the critical concentrations of impurities, for which the CDW ordering would be completely eliminated, and close to the critical temperature T_p, a perturbative expansion in terms of the order parameter Δ results in the equation of Landau-Ginzburg type[10]

$$\dot{\Delta} - iE\Delta - \partial_x^2\Delta - \partial_\perp^2\Delta - \Delta + |\Delta|^2\Delta = 0 \qquad (1)$$

The electric field is assumed here to be much larger than the bulk treshold field E_{tb}, so that the term describing the potential of random impurities is neglected (i.e. $E_{tb} \approx 0$ is assumed).

All quantities in eq.(1) are defined as dimensionless. The amplitude $|\Delta|$ of the order parameter $\Delta = |\Delta|\cdot\exp(i\phi)$ is measured in terms of its thermodynamic value $|\Delta_\infty|^2 = \frac{8}{5}\pi^2 T_p^2\delta$, where $\delta = 1-T^*/T_p^*$. The phase ϕ describes the modulation of the fast $2k_F$ wave form. The unit of the electric field E is $\pi^2 T_p^2\delta/6\overline{v_x}e$, while time and length units are defined by $\omega_0^{-1} = (27/16\pi^2)(T_p^0/T_p^2\delta)$ and the correlation lengths $\xi_{\parallel,\perp}^2 \sim \overline{v_x^2}/T_p^2\delta$, respectively. Here e is the electron charge, $\overline{v_x}$ is the mean Fermi velocity in the longitudinal (x) direction and T_p^0 is the critical temperature in the absence of impurity scattering.

The motion of the CDW induced by the electric drive along the

sample contributes to the current in the x direction. The total current is given by

$$j_\parallel = -\frac{\sigma_\parallel}{e}\frac{\pi^2 T_p^2\delta}{6\overline{v_x}}\left[E - \lambda|\Delta|^2 E + \frac{\varepsilon}{9}\varepsilon\lambda|\Delta|^2\dot{\phi}\right] \qquad (2)$$

The first term in this expression is just the normal current, with $\sigma_\parallel$ representing the high temperature ($T > T_p$) ohmic conductivity. The strength of the remaining CDW contributions is defined by the parameters $\lambda \sim T_p^2\delta/T_p^{02}$ and $\varepsilon = \overline{v_\perp^2}/\overline{v_x^2}$. The Landau-Ginzburg expansion in eq.(1) which is made under the requirement $T_p \ll T_p^0$ [10], is thus limited to the regime in which the electric current (2) is dominated by the normal contribution.

A simple translationally invariant solution of the eq.(1),

$$\Delta = \exp\int^t E(t')dt' \qquad (3)$$

represents a stationary flow of undeformed CDW, with a velocity determined by the competition between the external electric drive and the relaxation scatterings. Although simplified after neglecting smooth variations due to impurities, this solution is appropriate in the parts of the system which are free of obstacles. It will be modified, however, in their presence. Our further analysis is limited to the obstacles with potentials which are so strong that they can be approximated by a potential barrier of infinite height. Such obstacles can be incorporated into the problem (1,2) by defining app opriate boundary conditions for the CDW order parameter. Since an infinite

barrier inhibits temporal variations of the order parameter, one has

$$\Delta(\vec{r}_n,t) = \Delta(\vec{r}_n), \qquad (4)$$

where $\vec{r}_n$ represents symbolically a geometrical form of the n-th obstacle.

The integration of eq.(1) with the boundary condition (4), and in the presence of finite ac field will be limited here to the obstacles with extended transverse dimensions ($d_\perp \gg \xi_\perp$), mentioned already in the Introduction. In order to simplify the numerical procedure, we assume that the boundary (4) has the form of the plane perpendicular to the longitudinal direction. The solution $\Delta(r,t)$ then depends only on x, so that the term $\partial_x^2\Delta$ in the eq.(1) disappears. This class of one-dimensional solutions is expected to be appropriate in two opposite physical limits. The first one is that of strong transverse correlations, when $\xi_\perp$ is comparable to the transverse dimensions $d_\perp$ of the obstacles or of the sample itself. The roughness of the obstacles is then effectively smeared out, so that there is a coherent motion of the CDW throughout the corresponding cross section, described by the one-dimensional solution. In the opposite limit of weak transverse coupling, each narrow transverse domain of size $\xi_\perp \ll d_\perp$ can be considered separately and is described by the local (one dimensional) boundary conditions which follow the "morphology" of the obstacles.

A one-dimensional solution will be presumably modified for obstacles with boundary conditions varying on the scale comparable to $\xi_\perp$. Then the three-dimensional CDW correlations have to be taken into account, i.e. the separation of transverse and longitudinal dependence

is not possible. This more complex situation will be considered elsewhere[11]. We note only that, since there is no driving force and no CDW motion in a transverse direction, the transverse dependence of the order parameter is presumably slower than the longitudinal one, both in time and space. The main characteristics of the PS's, as highly nonlinear, dissipative process with strong and localized amplitude and phase variations, are expected therefore to remain qualitatively the same even in presence of transverse effects. This holds in particular for the harmonic content of the voltage originating from the time variations of the order parameter during the PS process.

The expression for the voltage is obtained after assuming the usual experimental conditions by which the total current through the sample is fixed. From the expression (2) for the current, one gets the local contribution to the electric field

$$\delta E(x,t) = \lambda\left[\,|\Delta|^2 E - \frac{\varepsilon}{\eta}\,\xi|\Delta|^2\dot{\phi}\,\right], \qquad (5)$$

which leads to the additional contribution to the sample voltage relative to that of the high temperature (ohmic) phase. For a given segment bounded by two adjacent obstacles, it is given by

$$\delta V(t) = \int_0^L dx\ \delta E(x,t), \qquad (6)$$

where the integration is to be performed over the segment length. Using the substitution

$$|\Delta|^2\dot{\phi} = |\Delta|^2 E + \partial_x(|\Delta|^2\partial_x\phi), \qquad (7)$$

which follows directly from the one-dimensional version of the eq.(1), the equation (6) reduces to

$$\delta V(t) = \lambda \left[(1 - \tfrac{8}{3}\varepsilon) \int_0^L |\Delta|^2 E \, dx - \tfrac{8}{3} \varepsilon \, (|\Delta|^2 \partial_x \Phi) \Big|_0^L \right] \qquad (8)$$

where the gradient terms depend on the actual boundary conditions (4) at the segment boundaries.

The electric field E in the eqs.(1) and (8) is the total electric field in the sample, which also selfconsistently includes the corrections (5). However, since $\lambda << 1$, the latter contribution is much smaller than the external field. Thus in the lowest order approximation, consistent with that which led to the eqs.(1) and (2), the electrical field E in the eq.(1) reduces to the space independent external field. Furthermore, the total current through the sample is also practically proportional to the external electric field, since it is determined dominantly by the ohmic contribution in the eq.(2). The one-dimensional solutions of eqs. (1) and (8) with $E \approx E_{dc}$ is analyzed in two stages.

In the first one we treat the case in which distances between the neighbouring barriers are much larger than the longitudinal CDW correlation length. Since the PS process is highly localized, each obstacle can be then considered separately. The order parameter is then practically unperturbed far from a given obstacle (at distances $L >> \xi_{||}$), so that the problem can be modeled as that of a semi-infinite system ($L \to \infty$) with the obstacle at one end and the free CDW motion at the other. The bulk contribution to the voltage (8), coming from the

free part where $|\Delta| = 1$ and $\dot{\Phi} = E$, just scales with L and can be subtracted from (8). By taking into account also that $\partial_x \Phi|_L = 0$ for $L \to \infty$[12], one gets from (8)

$$V_{PS} = \lambda \left[(1 - \tfrac{8}{3}\varepsilon) \int_0^L (|\Delta|^2 - 1) E \, dx + \tfrac{8}{3} \varepsilon \, |\Delta|^2 \partial_x \Phi \Big|_0 \right]. \qquad (9)$$

This is just the contribution to the sample voltage from the PS region.

In the next stage we include the effects of finite distance (2L) between two adjacent obstacles. The actual calculations are performed with the simplest assumption of symmetric boundary conditions at the segment boundaries[13]. The solutions $\Delta(x,t)$ are then symmetric with respect to the middle of the segment, so that $\partial_x \Phi|_L = 0$ and the expression (9) for the voltage still holds. As discussed in more details in Ref.[11], finite L leads to the treshold field ($E_t(L) \sim L^{-1.33}$) which competes with the bulk treshold. The effective electric field which defines the CDW current in the segment interior has to be measured from $E_t(L)$, i.e. the CDW current is suppressed with respect to the $L \to \infty$ case. The fundamental frequency of the PS's and the corresponding voltage in presence of dc fields is lowered therefore to the values $\omega_{ps}(L) = (E_0^2 - E_t^2(L))^{1/2}$.

3. NUMERICAL RESULTS

The problem (1,2) with the time dependent electric field

$$E(t) = E_0 + E_1 \cos(\omega_{ext} t + \varphi_0) \qquad (10)$$

can be treated analytically[19] only in the limit of large fields, $E_0 >> 1$ in the dimensionless units used here. As was already noted, the physical range of fields corresponds to the opposite limit, $E_0 << 1$, in which only numerical methods prove to be efficient. Since by decreasing the value of E_0 the needed computing time fastly increases, our calculations are limited to the fields $E_0 \leq 1$ ($E_0 = 0.5$ in most of our results). We believe that, like in the case of dc external fields[11], the solutions have all qualitative properties characterizing the regime of small fields already for these values. The boundary condition at fixed end is chosen to be $\Delta(x=0) = 1$. We put also $\varepsilon = 1$ in the eq.(9), and so fix the relative weight of the first and second term in eq.(5). This is not relevant for the overall conclusions, since both terms have similar qualitative behaviour.

3.1 SEMI-INFINITE SYSTEMS

We start by considering the limit of ac frequencies, small with respect to the intrinsic frequency of the PS process, $\omega_{ext} << \omega_{at}$. The

variations in time of the PS positions $x_{PS}(t)$, time intervals Δt_{PS} between two successive PS's and the PS voltage $\overline{V}_{PS}$ averaged over the corresponding Δt_{PS} are shown in Figs.1a,b,c respectively, for $\omega_{ext} = \omega_{at}/10$ and for two different values of ac amplitude, $E_1 = 0.05$ and 0.30.

As long as the amplitude of the ac field is small with respect to the dc field ($E_1/E_0 = 1/10$ in Fig.1, dashed line), all the above quantities are sinusoidally modulated with frequency ω_{ext} about the respective mean values x^0_{PS}, $2\pi/E_0$ and $\overline{V}^0_{PS}$ which characterize the system in absence of an ac field. This behaviour can be well understood in terms of the results obtained for dc fields. As the changes of the external field are slow with respect to the time intervals Δt_{PS}, the system behaves adiabatically, i.e. the PS positions and the corresponding voltage are in a good approximation determined by the electric field in the moment of the PS. They oscillate therefore within the values which correspond to the fields $E = E_0 \pm E_1$ in a dc case.

By increasing the ac amplitude E_1, the above modulations do not only increase in amplitude, but start also to deviate from the sinusoidal form. This nonsinusoidality is particularly evident for the PS voltage (Fig.1c, full line) which ceases to coincide with its "adiabatic" value, i.e. $\overline{V}_{PS}(t) \neq \overline{V}^0_{PS}(E(t))$. $\overline{V}_{PS}(t)$ corresponds now to some effective field which differs from E(t) in a way which depends not only on the amplitude, but also on the phase of the ac component in the moment of the PS. Simultaneously, the mean value of the PS voltage throughout the period of modulation starts to differ from its value for $E_1 = 0$ value. These effects become more and more pronounced by increasing also the value of ω_{ext}, i.e. by approaching the regime in which E_1,

ω_{ac1} and ω_{ac2} are comparable. In this regime one encounters resonance effects, which will be discussed in what follows.

Let us take at first the simplest case of the ac frequency and the fundamental frequency close one to another, $\omega_{ac1} \approx \omega_{ac2} \approx E_0$. The interplay of two frequencies is most directly evident in the Fourier spectrum of the induced PS voltage, depicted in Fig.2 for E_0=0.475 and ω_{ac1}=0.500, with E_1=0.30. The positions of discrete peaks are identified as the modulation frequencies $\omega_{nm} = |n\omega_{ac1} - m\omega_{ac2}|$, where n and m are integers. We emphasize particularly the low frequency peaks at $\Omega_1 \equiv \omega_{11} = |\omega_{ac1} - \omega_{ac2}|$ and its higher harmonics ω_{n1}, $n > 1$. They correspond to the modulation of the PS's in the time interval of the common periodicity of the internal PS production and the external ac drive. The modulations on the direct time scale of the PS position $x_{PS}(t)$, and PS periods Δt_{PS} for two symmetric values of dc fields about the resonant value, $E_0 = \omega_{ac1} \pm |\delta E_0|$ are shown in Fig.3a and b respectively. These modulations can be simply understood: due to the difference δE_0, the effective field which defines the PS behaviour changes from one PS to another through the time period of $\delta E_0^{-1} = \omega_{11}^{-1}$. We point out, however, the high nonsinusoidality of the modulation. As is evident from Fig.3a, the system passes quickly through the relative phases of the external field for which the PS's are most distant from the barrier, i.e. for which the effective field is weakest. This effect is associated with a tendency of the system to adapt to the periodicity of the driving field. As is shown in Fig.3b, this leads to the long time intervals in which the time Δt_{PS} between two slippages is $\Delta t_{PS} \approx 2\pi/\omega_{ac1}$. However, due to conservation of the charge, the mean interval $\langle \Delta t_{PS} \rangle$ throughout the period of modulation has to be E_0. The

compensation due to this mismatch is performed in short time intervals of only few PS's, for which Δt_{PS} is significantly shortened (for $E_0 > \omega_{ac1}$) or prolonged (for $E_0 < \omega_{ac1}$) with respect to $2\pi/\omega_{ac1}$. As is seen in Fig.3, there is some similarity in this compensation for two symmetric values of E_0 about ω_{ac1}. In contrast to that, the modulation of V_{PS} shown in Fig.4 is qualitatively different when the system is reaching or surpassing the ac periodicity. As will be shown later, this dependence of $\bar{V}_{PS}$ on the sign of δE_0 will lead to the finite step in the V_{PS} vs. E_0 curve at $\delta E_0 \approx 0$.

Modulations similar to that for $E_0 \approx \omega_{ac1}$ are found also close to the higher order resonant ratios $E_0/\omega_{ac1} = m/n \neq 1$. The $m/n > 1$ and $m/n < 1$ frequency ratios are usually distinguished as harmonic and subharmonic frequency ratios, respectively. For illustration, we consider the cases $E_0/\omega_{ac1} = 2$ and $E_0/\omega_{ac1} = 1/2$.

The time dependence of sample voltage for the frequency ratio close to the subharmonic value 1/2, E_0=0.26 and $\omega_{ac1}/2 = 0.25$ with E_1=0.30, is shown in Fig.5. We first note the influence of the driving field oscillations that modulate the order parameter behaviour within each particular PS period. However, after eliminating this "fast" ω_{ac1} component of the modulation, we find the slow voltage modulation with $\Omega_{1/2} = |\delta E_0| = |2E_0 - \omega_{ac1}|$, shown in Fig.6a. The highly nonsinusoidal voltage beats are associated again with a tendency of the PS's to favore some preferable range of relative phases of the ac field, and to avoid others. Once the preferable phase is achieved, the system tends to lock its periodicity onto the external ac field. Locking is interrupted only for relatively short time intervals of frequency accommodation. In these intervals the PS period Δt_{PS} increases , as is

shown in Fig.6b. The equivalent decrease of Δt_{PS} is realized at the opposite side of resonance. The asymmetry in the corresponding voltage modulations is again present, though it is much weaker than that for the fundamental resonance, m/n ≈ 1.

Fig.7 shows the voltage modulation for the dc field E_0=1.1 close to the harmonic value $2\omega_{ext}$=1.0. Since two successive PS's develop now in two half periods of the external ac field, the basic periodicity is defined by every second PS, i.e. by the driving frequency ω_{ext}. A modulation of V_{PS}, due to the deviation of E_0 from the exact resonant value, has the frequency $\Omega_1 = |E_0/2-\omega_{ext}|$. Compared to the case $E_0 \approx \omega_{ext}$, this modulation is more sinusoidal and, accordingly, the differences between two opposite sides of the resonance are less pronounced.

The common property of all three resonances considered above is the appearance of nonsinusoidal voltage modulations on passing through the resonant values of $\omega_{int}(E_0)$. Qualitatively the same , though weaker effects were found also at higher order harmonic and subharmonic resonances. The amplitude of these modulations and, in particular, differences in their behaviour at opposite sides of a given resonance, depend sensitively on the order of resonance and, for ω_{ext}=0.6 and E_1=0.3, become numerically scarcely detectable for n and/or m larger than 3. We note however, that these differences become more and more pronounced with the increase of the ac amplitude.

The above differences in the voltage $\bar{V}_{PS}$ lead to another important effect. Namely, the mean value of the PS voltage averaged over the period of modulation, $\langle V_{PS}\rangle$, displays finite steps when a given resonant value of field is approached from the opposite sides. These

steps are clearly seen in Fig.8 at the lowest order resonant ratios n/m = 1, 2 and 1/2, for two values of the external frequencies, ω_{ext}=0.50 and ω_{ext}=0.25, and for the ac amplitude fixed at E_1=0.30. Note that the step height at a given resonant ratio n/m significantly weakens as the ratio E_1/ω_{int} decreases. Comparing Fig.8 with the previous results, it becomes clear that the steps in the $\langle V_{PS}\rangle$ vs E_0 dependence are a direct consequence of the discontinuities in the voltage modulations at the commensurate ratios of $\omega_{int}/\omega_{ext}$. The height of a given step depends on the strength of corresponding discontinuity, which decreases as n and/or m in the resonant ratio n/m increases. The steps of the order higher than those indicated in Fig.8 are at or beyond the level of our numerical resolution, and are therefore not clearly visible for the considered value of ac amplitude.

The dependence of the step heights on the ac amplitude E_1 is shown in Fig.9 for E_0/ω_{ext} = 1 and 2. The step height is here defined as a difference $\delta\langle V_{PS}\rangle$ of the values $\langle V_{PS}\rangle$ at the dc fields E_0 which are 20% larger and smaller than the given resonant value $E_{0,res}$. $\delta\langle V_{PS}\rangle$ oscillates as a function of E_1, with the amplitude which decreases as E_1 increases. The period of these oscillations, when scaled with ω_{ext}, coincides with the analytical results in the limit of large electric fields[11]. We have not analyzed in details a dependence of $\delta\langle V_{PS}\rangle$ on ω_{ext}. Possible modifications of this dependence in the regions of small frequencies, i.e. of dc fields close to the treshold field, cannot be excluded. Such departure from the linear scaling with ω_{ext} is actually observed at low frequencies in the experiments of Thorne at al.[3] on $NbSe_3$ samples. A comparison of our results with the experiments is therefore limited to higher frequencies, i.e. to resonant fields not

close to the treshold field.

As an example we compare the characteristic rate of the oscillations of the step heights with E_1 obtained from our results, with that one observed at $\omega_{ext}/2\pi$ = 5MHz in the experiments of Thorne et al.[3]. The corresponding resonant value of dc voltage is about 50 mV, in comparison to $V_t \approx 16$ mV, and belongs to the range of linear scaling with ω_{ext}. The position of first maximum for e.g. 1/1 resonance is at $V_{dc}/V_t \approx 5$. For the sample of length of 2.8 mm, this corresponds to $E_1/\omega_{ext} \sim 0.9\cdot10^{-6}$ V/ms^{-1}. In order to compare this result with ours, let us remind that a physical unit of our dimensionless ratio E_1/ω_{ext} is $(32\pi/9\pi)\cdot ev_F E_1/k_B T_P^2 \omega_{ext}$. Using the values $\xi \sim \hbar v_F/k_B T_P \sim 1.5\cdot10^{-6}$ cm and $2\Delta/k_B T_P \sim 3.5 T_P^0/T_P \sim 12$, typical for the transition metal trichalcogenides[1], the position of the first maximum is estimated at $E_1/\omega_{ext} \sim 0.5\cdot10^{-6}$ V/ms^{-1}, in good agreement with the above experimental value[3].

We turn now to some details of the step structure, by considering as an example the fundamental step at $\omega_{ext} = \omega_{NBN}$. Exactly in the resonance the modulation frequency passes through zero, i.e. the system stabilizes itself after few slippages, so that the successive PS's occur at some fixed relative phase with respect to the external ac field. For small ac amplitudes ($E_1 \ll E_0$) this phase may have any value between 0 and 2π, depending on the initial phase φ_0 in eq.(10), i.e. on the value of an ac field in the moment of its switching. However, by increasing the ac amplitude, a width of the band of "stable" phases $\delta\varphi$ gradually decreases, becoming very narrow ($\delta\varphi \ll 2\pi$) for $E_1 \sim E_0$. The corresponding range of the allowed PS positions also decreases and shifts towards the barrier. Even then however, the system "memorizes"

the initial phase φ_0, so that the value of the averaged PS voltage depends on this phase. The allowed values of $\langle V_{PS}\rangle$ span a finite band with the width which coincides with the limiting amplitude of the voltage modulations for $E_0 \sim \omega_{ext}$, i.e. surpasses the step height defined by extrapolation of $\langle V_{PS}(E_0)\rangle$ from outside the resonance. The origin of this singular behaviour of the otherwise continuous curve $\langle V_{PS}(E_0)\rangle$ is to be associated with an additional effect of approaching the resonance, namely the increase of the CDW phase gradient $\partial_x\varphi|_{x\to L_\infty}$ far away from the barrier. This indicates that the PS process becomes less and less local in the vicinity of resonance and at the resonance itself, so that the effects of finiteness of segments between two barriers become particularly important.

2.2 FINITE SIZE EFFECTS

It has been mentioned already in Sec.2, that the interference between the PS's from the adjacent obstacles leads to the shift of the fundamental NBN frequency towards lower values, which depend on the segment length[11]. Thus the resonant value of the dc field E_0 in the ac-dc coupling regime will be shifted towards the higher value, given by the condition

$$n\omega_{NBN}(L) = n\cdot(E_0^2 - E_t^2(L))^{1/2} = m\omega_{ext}. \qquad (11)$$

The numerical results for finite values of L show that, outside from the resonance regions, the PS process and the corresponding voltage remain the same as in the $L \to \infty$ limit. Qualitative changes are,

however, found in the very vicinity of the resonances.

Fig.10 shows the behaviour of the modulation frequency Ω_1 close to the fundamental resonance for finite value of L (L=20). By approaching the exact resonant value from either side, the initially linear dependence of $\Omega_1(E_0)$ on the relative frequency $|\omega_{st}-\omega_{ext}|$ bends towards zero. In a finite region of dc fields ΔE_0 around the resonant value defined by the eq.(11), there is no additional modulation of the PS's due to the ac field. After few periods of initial adjusting, the phase of the PS oscillations relative to the ac field remains stabilized at a fixed value. The band of such stable phases for different values of dc fields within ΔE_0 coincides with the band $\delta\varphi$ of allowed phases for the semi-infinite system at the resonance. Thus both the frequency and the phase of the PS oscillations become locked, i.e. the complete mode locking onto the external ac field is achieved in the region ΔE_0. This is a finite size effect. The numerical dependence of the width ΔE_0 on L which is shown in Fig.11, suggests the asymptotic law

$$\Delta E_0(L) \sim L^{-1} \qquad (12)$$

for sufficiently large values of L.

The comlete mode locking influences also the structure of Shapiro steps. Fig.12 shows the fundamental step for two finite segment lengths, L=10 and L=20, compared with the $\langle V_{PS}(E_0)\rangle$ behaviour for the semi-infinite system ($L \to \infty$). The most important feature is the appearence of regions of negative differential resistance $d\langle V_{PS}\rangle/dE_0$ for finite values of L. Comparing Fig.12 with Figs.10 and 11, it becomes clear that the regions of fields enclosed by the negative wings

in $d\langle V_{PS}\rangle/dE_0$ coincide with the mode locking widths $\Delta E_0(L)$. Narrowing of ΔE_0 with L (Fig.11) explains therefore the singular behaviour of $\langle V_{PS}(E_0)\rangle$ at $\omega_{st} = \omega_{ext}$ in the semi-infinite system.

We note that negative "wings" in dV/dI vs. I curves are unusually observed experimentally[6] in samples which display complete mode locking. A dependence of mode locking width on L and, in particular, the singularity for $L \to \infty$ can be however smeared out in the experiments, due to a finite distribution of ω_{st} in physical samples.

Let us note again that, except for the shifts of the resonant frequencies, the finite size effects are not found outside from the resonant regions. The step heights, defined from outside the resonances, are therefore uniquely determined by the external field parameters E_1 and ω_{ext}/ω_{st}. This conclusion is, however, limited to the lengths $L >> x_{PS}$ for which PS minima at two ends do not overlap. The correspondent mode locked regions are still narrow in comparisson to the distance between the numerically detectable resonances on E_0 scale. In the limit of very short segments, or of large ac amplitudes, in which the higher order resonances become also appreciable, the overlap of neighbouring mode locked regions may lead to more complicated structure of steps.

4. DISCUSSION

The central result of the above numerical analysis is the appearance of steps in the curves shown in Fig.8, i.e. in the dependence of the averaged CDW voltage on the external dc field. Steps are found at harmonic and subharmonic ratios of the frequencies of the internal ($E_1=0$) voltage oscillations and of the external ac field. They are the consequence of the anomaly in the average voltage with respect to the sign of the frequency difference $n\omega_{ext}-m\omega_{int}$, which in turn results from the discontinuity in the modulation of the CDW current (and of the corresponding time dependent voltage) at a given resonance. Note that the E_0 and $\langle V_{PS}\rangle$ axis in Fig.8 correspond respectively to the bias dc current and dc voltage in usual experimental curves.

Both, harmonic and subharmonic resonances are generally expected in a wide class of nonlinear systems with mixing of internal oscillations and the external periodic drive. E.g., the classical model of rigid CDW shows this property after assuming a nonsinusoidal form of the effective potential[24,28], or after including the inertial term $\ddot{\phi}$ [28] into the equation of motion for the CDW phase. The analysis of nonlinear I-V characteristics[3], claimed to be an appropriate description of quantum CDW tunneling[27], also shows the appearance of both resonances. The essential step in both mentioned approaches, is the elimination of spatial coordinates, i.e. the assumption that space scales responsible for the interferences are large, at least of the order of Lee-Rice domains. The microscopic averaging procedure is usually substituted by a phenomenological choice of effective

nonlinear potentials (or current-field relations), aimed to fit satisfactorily experimental data.

In contrast to bulk resonances in these approaches, the nonlinear mixing in Gor'kov's model takes place in particular parts of system, localized close to obstacles and characterized by the length x_{PS}. The dynamical equation (1) which includes space variations is obviously mathematically more complex than those appearing in models with a single degree of freedom. Since the numerical integration of this equation takes a considerable amount of the computation time, we had to limit severely the analysis on the dependence of Shapiro steps on the external field, i.e. on E_0 and E_1. As is seen in Sec.3., qualitative trends, recognized in obtained numerical solutions, are in agreement with experiments. On the other hand, these solutions give a detailed description of the PS diffusion at and close to the resonances. This enables the understanding of some effects which are beyond the rigid CDW models, and are connected with the finiteness of longitudinal and transverse scales relevant for CDW dynamics in presence of obstacles. The rest of this section is devoted mainly to these questions.

The effects of sample finiteness are absent in the semi-infinite system examined in Sect.3.1. The Shapiro steps have no width on E_0 scale, so that complete mode locking, i.e. the perfect accommodation of the system to the frequency ω_{ext} and the relative phase φ of the external field (10) is accomplished only for $n\omega_{ext} = m\omega_{int}$. As is shown numerically, the band of relative phases to which the system can lock is rather narrow ($\delta\varphi \ll 2\pi$). Due to this, the modulation of $x_{PS}(t)$ and $V_{PS}(t)$ close to resonances has a characteristic kink-like shape (Fig.4). Effectively, the system is not locked only during short

intervals of beats or "discommensurations" on time scale. These beats lead to side peaks in the Fourier spectrum (Fig.3).

The Shapiro steps of finite width, i.e. the mode locking in finite regions of ΔE_0 (or ω_{osc}) is a size effect, as is shown in Fig.11. The finiteness of the system becomes important when the tails of PS diffusion from the opposite ends start to interfere. The interference is particularly enhanced at resonances, since then the PS diffusion penetrates more deeply into the interior of the system[19]. Being mutually coherent, the PS's from the two ends may avoid their own temporal discommensurations, so that the complete locking becomes possible for finite values of $n\omega_{osc} - m\omega_{sl}$, i.e. within the finite length dependent range ΔE_0 given by the eq.(12). This effect is accompanied by the formation of wings at both sides of a given Shapiro step. The finite length scale, i.e. the nonrigidity of CDW, is crucial for these results.

The above conclusions may be now extended to more involved situations, closer to those realized in experimental specimens.

Let us assume at first that the specimen of length L is divided by strong obstacles into N segments which are mutually independent. The n-th segment is characterized by a value of electric field E_n measured with respect to the local treshold electric field, i.e. by its own resonant frequency $\omega_{sl,n}$ and relative phase φ_n of PS oscillations. The latter is imposed by boundary conditions for this segment. A distribution of resonant frequencies, characterized by some mean deviation δE, (i.e. $\delta\omega_{sl}$) leads to finite width of NBN peaks, which is still very narrow in specimens of good quality. On the other hand, due to random distribution of phases for N segments, the total NBN

amplitude is reduced with respect to the coherent system. E.g. for large N it is proportional to $N^{1/2}$, instead of N.

With the ac field switched on, the condition of resonance, $n\omega_{osc} = m\omega_{sl,n}$ cannot be achieved in all segments, provided that they are long enough. However, at a given moment, most of the segments is locked to the ac field, which also imposes a common relative phase of the oscillations. Among the segments which are not in the strict resonance, only a small part will at this moment accommodate PS oscillations through beats. The contribution of such incoherent beats from different segments to the total averaged voltage (and to the discontinuities in Shapiro steps) is therefore even weaker than in the case of a perfectly coherent system. Thus, unlikely to the NBN amplitude, the heights of the steps will remain proportional to N (i.e. L). This explains different length dependences of these two quantities, observed in some measurements[15,16,17] on $NbSe_3$. The step widths scale with the field distribution, like the widths of frequency peaks in NBN.

The synchronization in the ac field is even more efficient for short segments which are locked in finite field ranges ΔE_n (eq.(12)). A complete mode locking may be realized in the entire specimen, provided that the overlap of these widths is larger than the distribution of resonant frequencies $\delta\omega_{sl}$. The small changes of the externally biased dc current then go exclusively through the ohmic conduction, i.e. the differential resistivity assumes its low field (ohmic) value. Both, incomplete and complete mode locking is observed experimentally[28,29,30,3].

More realistically, one should expect that the segments are not completely decoupled and, even more, that they are not very well defined. The CDW coherence may partially persist in effective domain boundaries formed due to distorting forces from the sample inhomogeneity and anisotropy, thermal gradients etc. The PS oscillations in different parts of sample do not remain independent, though they can have considerably different frequencies (e.g. in experiments with imposed thermal gradients). The more appropriate boundary conditions are then those imposing different CDW velocities at two sides of a given boundary. In that case, the NBN contains low frequency peaks proportional to the difference of velocities, in addition to high frequency peaks which originate from strong obstacles and are proportional to local values of dc field. Such NBN spectra were observed in thermal gradient experiments[21].

The mode locking effects in the finite ac field might overcome these "weak" boundary conditions by synchronizing adjacent domains. With the increase of ac field amplitude E_1 the low frequency peaks will move towards smaller frequencies and eventually disappear. Simultaneously, widths of peaks at higher frequencies will gradually decrease. Note that in this interpretation the original configuration of domains still persists, in spite of apparent impressions that a new, ac field-induced, coherence length appears, and that a multidomain structure is reversed into a single domain one[28]. The synchronization of domains is caused by the individual locking of each particular domain onto the ac field, present only at and close to resonant values of ω_{res}. Outside the resonances, the sample response remain incoherent. This is clearly seen in e.g. the regime of weak and low frequency ac

fields, in which the NBN amplitude is adiabatically modulated, as was discussed in Section 3. (Fig.1). Details of current oscillations, i.e. of the sample coherence, remain present in this modulation. This agrees with the results of ac-dc coupling measurements[21] on $NbSe_3$, where the amplitude and frequency widths of low-frequency and side peaks in NBN spectra, corresponding to the above modulations, are shown to reflect the quality of the original ($E_{ac} = 0$) spectra.

5. CONCLUSIONS

The results obtained in this work follow from two basic properties of the PS process, its multiharmonic periodicity in time and its locality in space. The former property leads to discontinuities (Shapiro steps) at harmonic and subharmonic frequency ratios, and to beats in the voltage in the vicinity of resonances. The finite spatial extension of PS diffusion and the interference of adjacent PS's are responsible, when superimposed over the entire sample, for mode locking, step wings and synchronizations. The latter effects are of semi-macroscopic nature and are to a great extent sample dependent.

Having the points mentioned above in mind, we emphasize the necessity of simultaneous treatment of both space and time variations occurring in the PS diffusion[23]. This is possible in Gor'kov's model which covers systems with small relaxation times and dominating contribution of normal carriers to the ohmic transport. The equations (1,2) are based on the Landau-Ginzburg expansion, and therefore keep the microscopic meaning only for length and time scales respectively larger than the correlation lengths $\xi_{\parallel}, \xi_{\perp}$ and the time unit defined in Sec. 2. The scales relevant for the results of this work satisfy this requirement. Very fast and sharp variations characterizing the amplitude collapse in the phase slip are only a substitute for an essentially quantum process, considered in details in Refs. [34] and [35].

The actual numerical calculations are limited to the rather simple case of one-dimensional boundary conditions introduced in Section 3.

Two extensions to more complicated obstacles are particularly important for better understanding of NBN and resonances in samples with strong point defects, irregular boundaries and contacts, etc. The first one, mentioned already in Introduction, concerns the PS's at small (point) barriers. The second one again applies mostly to macroscopic barriers, and is connected with the microscopic nature of CDW dislocation lines, usually treated phenomenologically[36]. Both problems are under current investigations.

Acknowledgements

One of us (A.B.) acknowledges the hospitality of Professor Abdus Salam, IAEA and UNESCO, and Professors Yu Lu and E. Tosatti, organizers of the workshop "Non-linear CDW systems" at ICTP in Trieste. The work was supported in part by the Yu-US collaboration program DOE JF 738.

REFERENCES

[1] For general reviews see e.g. P.Monceau, in Electronic Properties of Inorganic Quasy One Dimensional Materials II, p.139-268, ed. P.Monceau, D.Reidel Pub.Comp. (1985) and G.Grüner and A.Zettl, Phys. Reports 119, 117 (1985)

[2] A.Zettl and G.Grüner, Solid St. Comm. 46, 501 (1983); Phys. Rev.B29, 755 (1984)

[3] R.E.Thorne, W.G.Lyons, J.W.Lyding, J.R.Tucker and J. Bardeen, Phys.Rev.B35, 6348 (1987), Phys.Rev.B36, 6360 (1987)

[4] K.B.Efetov and A.I.Larkin, Zh.Eksp.Teor.Fiz. 72, 2350 (1977) [Sov.Phys. JETP 45, 1236 (1977)]

[5] H.Fukuyama and P.A.Lee, Phys.Rev.B17, 535 (1977)
P.A.Lee and T.M.Rice, Phys.Rev.B19, 3970 (1979)

[6] G.Grüner, A.Zawadowski and P.M.Chaikin, Phys.Rev. Lett. 46, 511 (1981)

[7] P.Monceau, J.Richard and M.Renard, Phys.Rev.B25, 918 (1982); Phys.Rev.B25, 931 (1982)

[8] L.Sneddon, Phys.Rev.B 29, 719 (1984)

[9] P.A.Lee, T.M.Rice and P.W.Anderson, Solid St.Comm.14, 703 (1974)
N.P.Ong and K.Maki, Phys.Rev.B32, 6582 (1985)

[10] L.P.Gor'kov, Pis'ma Zh.Eksp.Teor.Fiz.38, 76 (1983) [Sov Phys. JETP Lett.38, 87 (1983); Zh.Eksp.Teor.Fiz. 86, (1984) [Sov.Phys. JETP 59, 1057 (1985)

[11] I.Batistić, A.Bjeliš and L.P.Gor'kov, J.Physique 45, 1049 (1984)

[12] P.A.Yetmann and J.C.Gill, Solid State Comm.62, 201 (1987)
J.Chen, M.C.Saint Lager and P.Monceau, Proc. Sec. European Workshop on CDW, Aussois 1987, p.14

[13] G.Mihaly and P.Beauchene, Solid St.Comm.63, 911 (1987)

[14] N.P.Ong and G.Verma, Phys.Rev.B27, 4495 (1983)

[15] N.P.Ong, G.Verma and K.Maki, Phys.Rev.Lett.52, 663 (1984)

[16] T.W.Ying and N.P.Ong, Phys.Rev.B33, 5841 (1986)

[17] G.Mozurkewich and G.Gruner, Phys. Rev. Lett. 51, 2206 (1983);
G.Mozurkewich, M.Maki and G.Gruner, Solid St. Comm.48, 453 (1983);
S.E.Brown and L.Mihaly, Phys.Rev.Lett. 55 (1985)

[18] R.P.Hall, M.F.Hundley and A.Zettl, Phys.Rev.Lett.56, 2399 (1986)

[19] A.Bjeliš and D.Jelčić, J.Physique Lett.46, 283 (1985)

[20] D.Jelčić and A.Bjeliš, I.Batistić, X Yugoslav Conference on Solid State Physics, Sarajevo 1986 (Fizika, Zagreb, to be published)

[21] A.Bjeliš, to be published

[22] In the numerical calculations the limit $L\to\infty$ is replaced by a finite length L_∞ for which the asymptotic, L_∞-independent, behaviour of the order parameter in the PS region is already achieved. As an artefact of this approximation, one obtains finite values of $\partial_x\phi/_{x\to L_\infty}$ and of the corresponding term in eq.(8), which will be skipped from the results presented in Sec.3.

[23] The numerical results of Ref.[11] for dc fields show that more general (asymmetric) boundary conditions do not change qualitative fetures of the PS process, in particular the periodicity of the PS oscillations.

[24] H.Matsukawa and H.Takayama, Synthetic Met. 19, 7 (1987)

[25] S.N.Coppersmith and P.B.Littlewood, Phys.Rev.Lett.57, 1927 (1986)

[26] P.Bak, Proc.Int.Symp. on Nonlinear Transport and Related Phenomena in Organic Quasi One Dimensonal Conductors, Sapporo, 1983, Japan, p.13

[27] J.Bardeen, Phys.Rev.Lett.45, 1978 (1980)

[28] R.P.Hall and A.Zettl, Phys.Rev.B30, 2279 (1984)

[29] M.S.Sherwin and A.Zettl, Phys.Rev.B32, 5536 (1985)

[30] X.J.Zhang and N.P.Ong, Phys.Rev. B30, 7343,(1984)

[31] M.C.Saint Lager, M.Prester, P.Monceau and M.Renard, Proc. Sec. European Workshop on CDW, Aussois 1987, p.30

[32] J.P.Stokes, S.Bhattacharya and A.N.Blooh, Phys.Rev.B34, 8944 (1986)

[33] The purely phenomenological model in which the space scale for the PS is reduced to an effective problem of single degree of freedom is proposed recently by M.Innui, R.P.Hall, S.Doniach and A.Zettl, to be published

[34] I.Tutto and A.Zawadowsky, Phys.Rev. B32, 2449 (1985)

[35] S.N.Artemenko, A.F.Volkov and A.N.Kruglov, Zh.Eksp. Teor.Fiz.91, 1536 (1986)

[36] J.Dumas and D.Feinberg, Europhys.Lett.2, 555 (1986) D.Feinberg and J.Friedel, "Low-dimensional properties of molybdenum bronzes and oxides", ed. C.Schlenker, D.Riedel Publ. Comp., 1988.

FIGURE CAPTIONS

Fig.1. Time dependence of PS variables for E_0 = 0.5, ω_{ext} = 0.05 and E_1 = 0.05 (Δ) and 0.3 ($\circ$): (a) The position $x_{PS}(t)$, (b) time intervals Δt_{PS} between two succesive PS's and (c) the averaged voltage $\overline{V}_{PS}$ divided by parameter λ (see eq.9))

Fig.2 The Fourier spectrum of the PS voltage $V_{PS}(t)$ close to the fundamental resonance, for E_0 = 0.475, ω_{ext} = 0.50 and E_1 = 0.30. Modulation peaks are defined by $\omega_{mn} = |n\omega_{ext} - m\omega_{int}|$

Fig.3 The modulations of (a) PS positions $x_{PS}(t)$ and (b) PS periods Δt_{PS} for E_1 = 0.3, ω_{ext}=0.5 and for two opposite values of dc field close to the resonant value: E_0 = 0.475 (solid symbols) and E_0 = 0.525 (open symbols).

Fig.4 PS voltage V_{PS} averaged over each particular PS period for two values of dc fields symmetric with respect to the resonant value ω_{ext} = 0.50: E_0 =0.475 (solid circles) and E_0 = 0.525 (open circles)

Fig.5 PS voltage V_{PS} vs. time close to the subharmonic resonant ratio 1/2, i.e. for E_0 = 0.26, ω_{ext} /2 = 0.25 and E_1 = 0.3.

Fig.6 The averaged voltage $\overline{V}_{PS}$ (a) and the PS periods Δt_{PS} (b) for parameters of Fig.5.

Fig.7 The averaged PS voltage $\overline{V}_{PS}$ close to the second harmonic resonance for E_0 = 1.1, $2\omega_{ext}$ = 1.0 and E_1 = 0.30. The basic periodicity is defined by every second PS. Dashed lines are the envelope of the modulation.

Fig.8 The mean value of the PS voltage throughout the periods of modulatins, $\langle V_{PS} \rangle$ vs. dc field, for $\omega_{ext} = 0.50$ (•) and $\omega_{ext} = 0.25$ (○). The positions of steps in $\langle V_{PS} \rangle$ are indicated by the arrows.

Fig.9 Heights of the steps in $\langle V_{PS} \rangle$ at $E_0 = \omega_{ext}$ (open circles) and $E_0 = 2\omega_{ext}$ (solid circles) vs ac amplitude E_1 for $\omega_{ext} = 0.25$.

Fig.10 Bending of the modulation frequency $\Omega_1(E_0)$ by approaching the fundamental resonance ($\omega_{1st}(L) \approx \omega_{ext} = 0.5$) for finite length L=10 and for $E_1 = 0.3$.

Fig.11 Dependence of the mode locking width ΔE_0 (Fig.10) on the inverse segment length 1/L.

Fig.12 Structure of the fundamental step at $\omega_{ext} = 0.5$ for L = 10 (open circles) and L = 20 (solid circles). The correspondent $\langle V_{PS} \rangle$ vs E_0 dependence for $L \to \infty$ is indicated by dashed line.

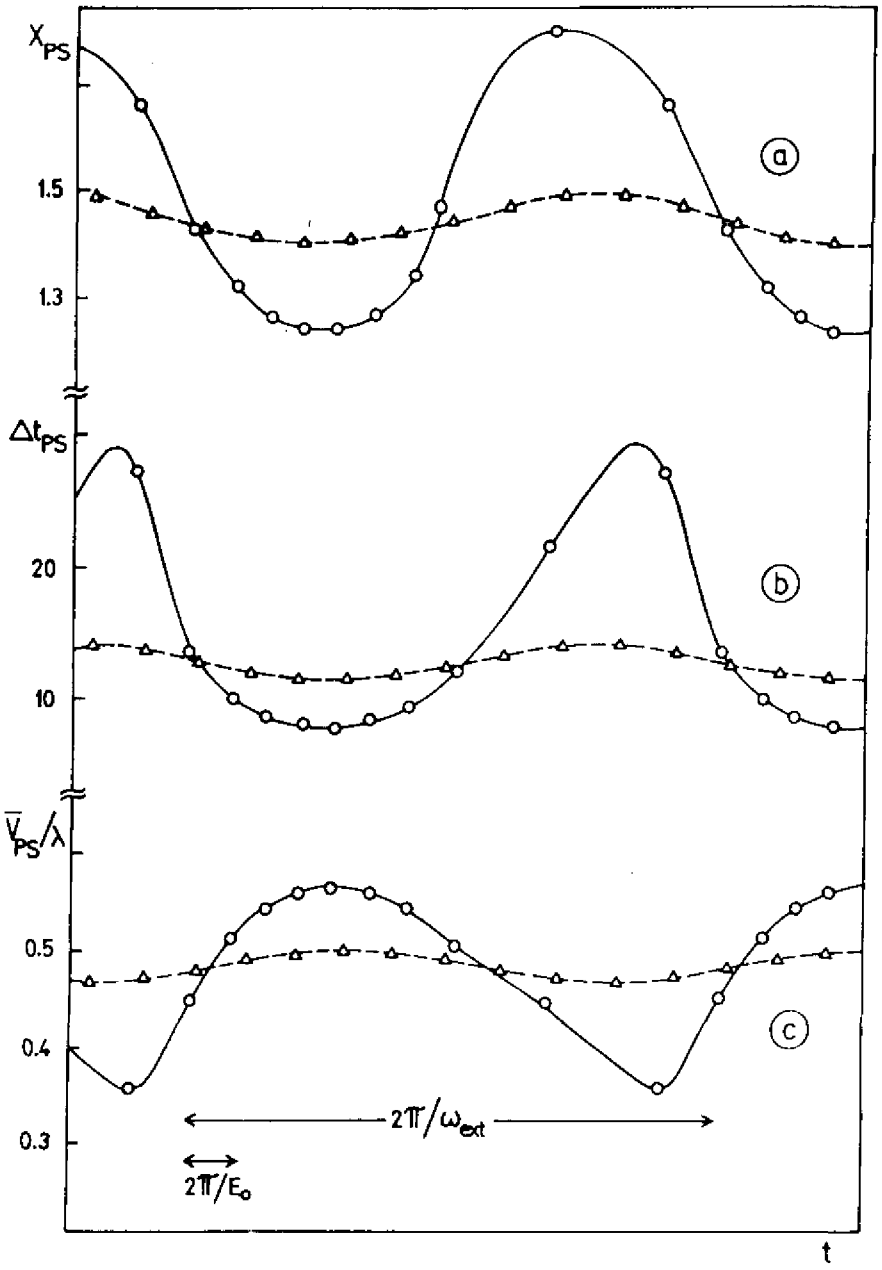

Fig. 1

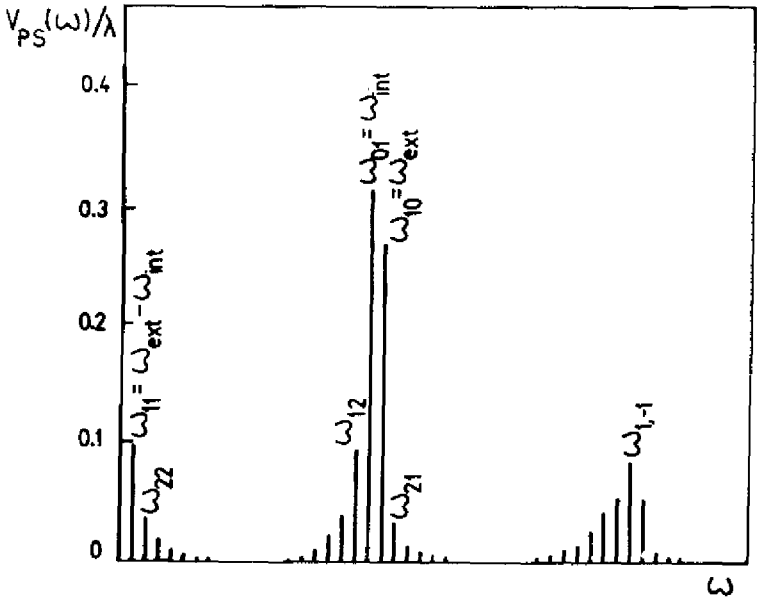
$V_{PS}(\omega)/\lambda$
0.4
0.3
0.2
0.1
0
$\omega_{11}=\omega_{ext}-\omega_{int}$
ω_{22}
ω_{12}
$\omega_{01}=\omega_{int}$
$\omega_{10}=\omega_{ext}$
ω_{21}
$\omega_{1,-1}$
ω

Fig. 2

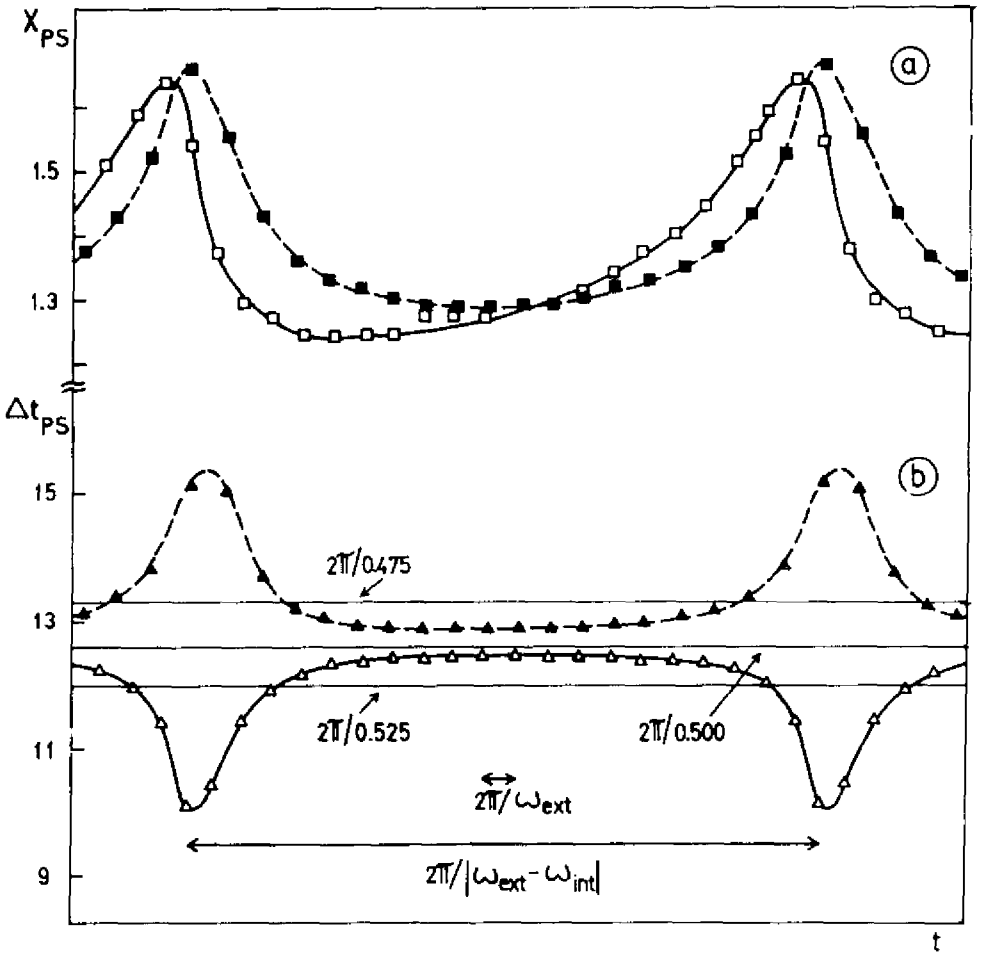
X_{PS}
1.5
1.3
Δt_{PS}
15
13
11
9
a
b
$2\pi/0.475$
$2\pi/0.525$
$2\pi/0.500$
$2\pi/\omega_{ext}$
$2\pi/|\omega_{ext}-\omega_{int}|$
t

Fig. 3

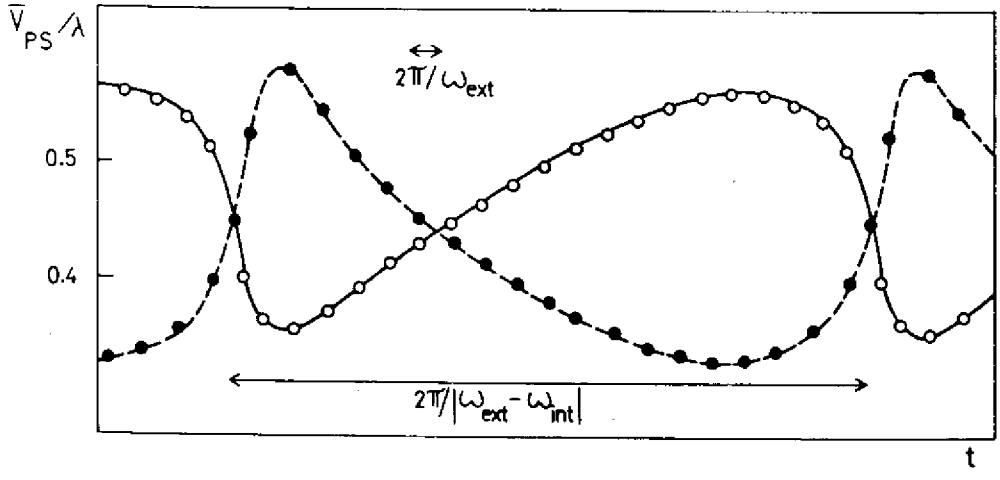
$\bar{V}_{PS}/\lambda$
0.5
0.4
$2\pi/\omega_{ext}$
$2\pi/|\omega_{ext}-\omega_{int}|$
t

Fig. 4

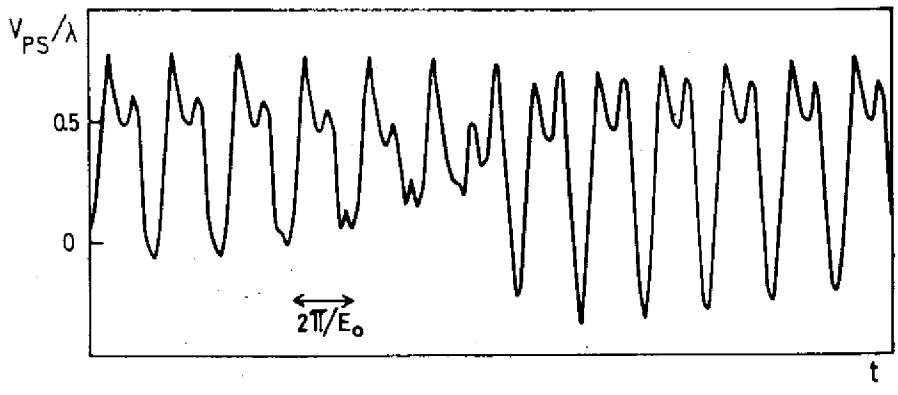
V_{PS}/λ
0.5
0
$2\pi/E_o$
t

Fig. 5

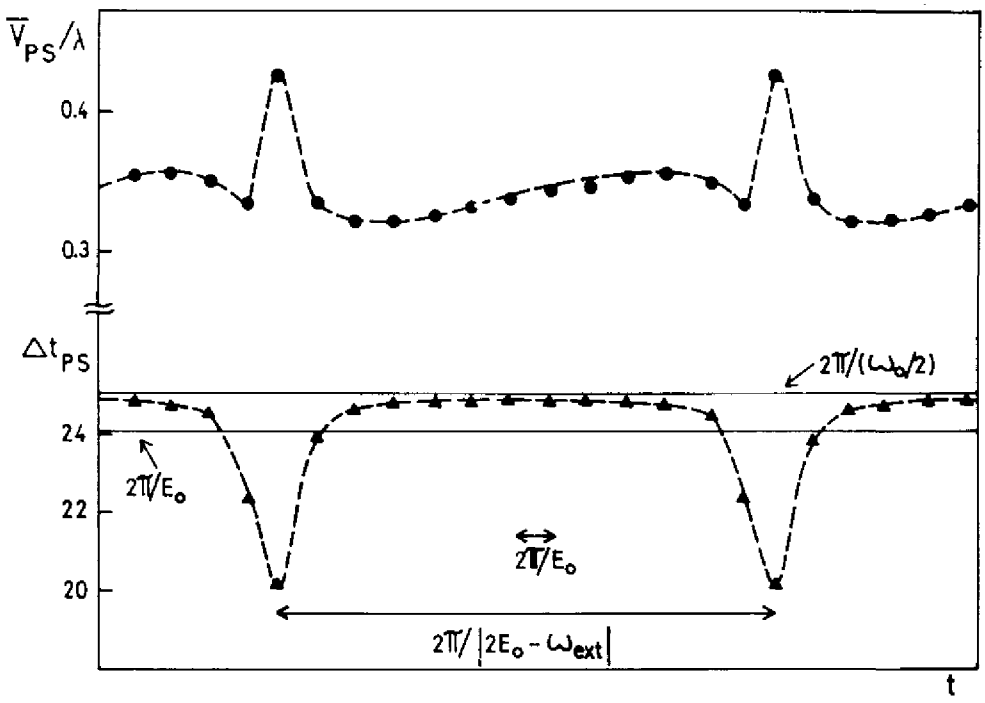
$\overline{V}_{PS}/\lambda$
0.4
0.3
Δt_{PS}
$2\pi/(\omega_o/2)$
24
22
20
$2\pi/E_o$
$2\pi/E_o$
$2\pi/|2E_o - \omega_{ext}|$
t

Fig. 6

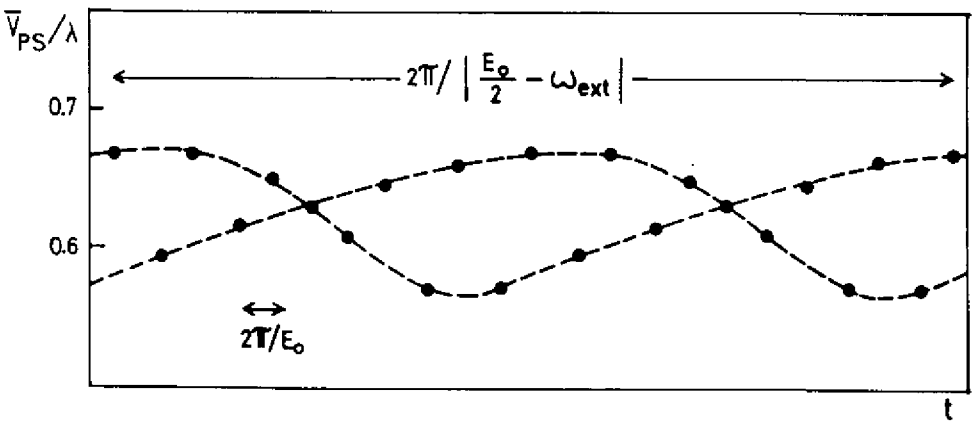
$\overline{V}_{PS}/\lambda$
$2\pi/\left|\frac{E_o}{2} - \omega_{ext}\right|$
0.7
0.6
$2\pi/E_o$
t

Fig. 7

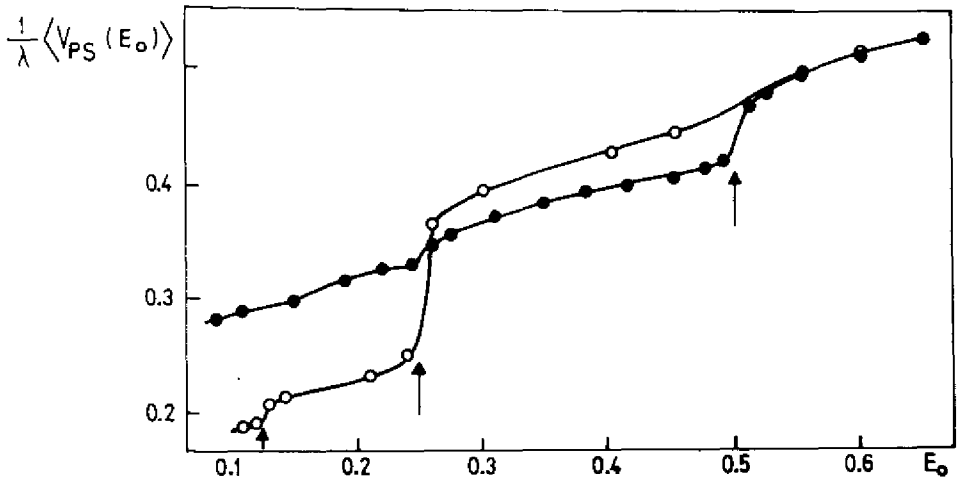
$\frac{1}{\lambda}\langle V_{PS}(E_o)\rangle$
0.4
0.3
0.2
0.1
0.2
0.3
0.4
0.5
0.6
E_o

Fig. 8

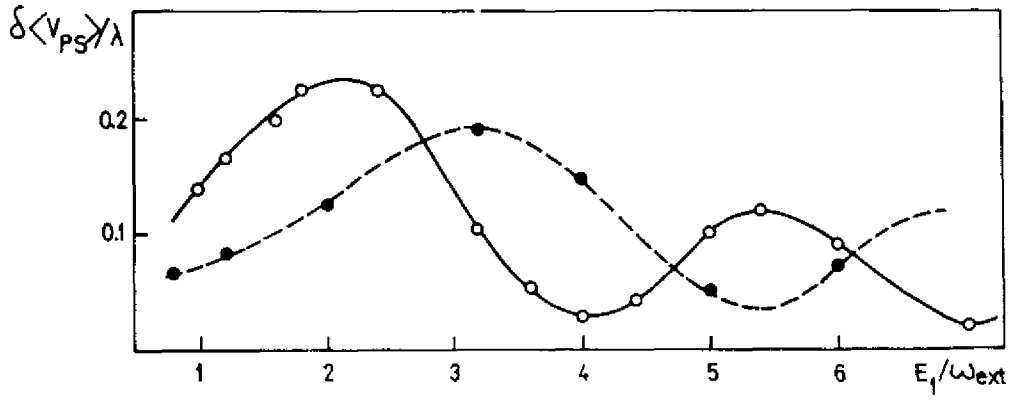
$\delta\langle V_{PS}\rangle/\lambda$
0.2
0.1
1
2
3
4
5
6
E_1/ω_{ext}

Fig. 9

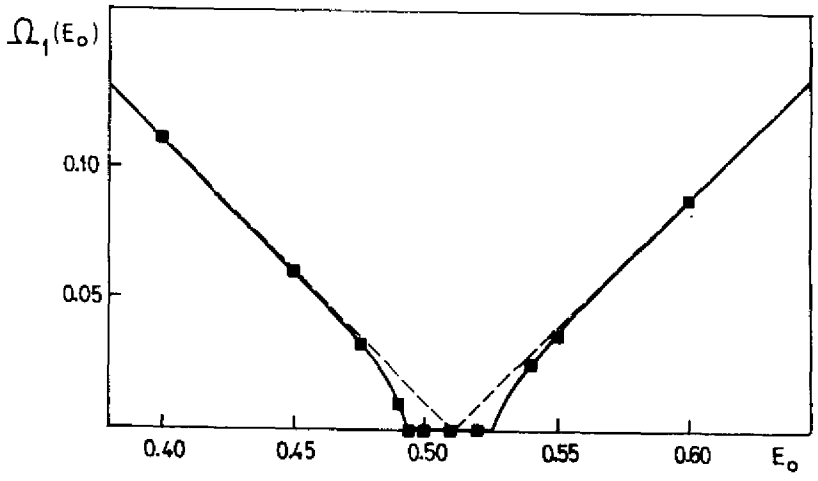
$\Omega_1(E_o)$
0.10
0.05
0.40
0.45
0.50
0.55
0.60
E_o

Fig. 10

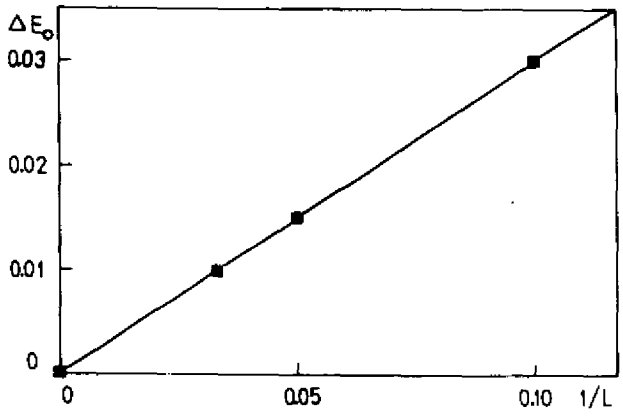
ΔE_o
0.03
0.02
0.01
0
0
0.05
0.10
1/L

Fig. 11

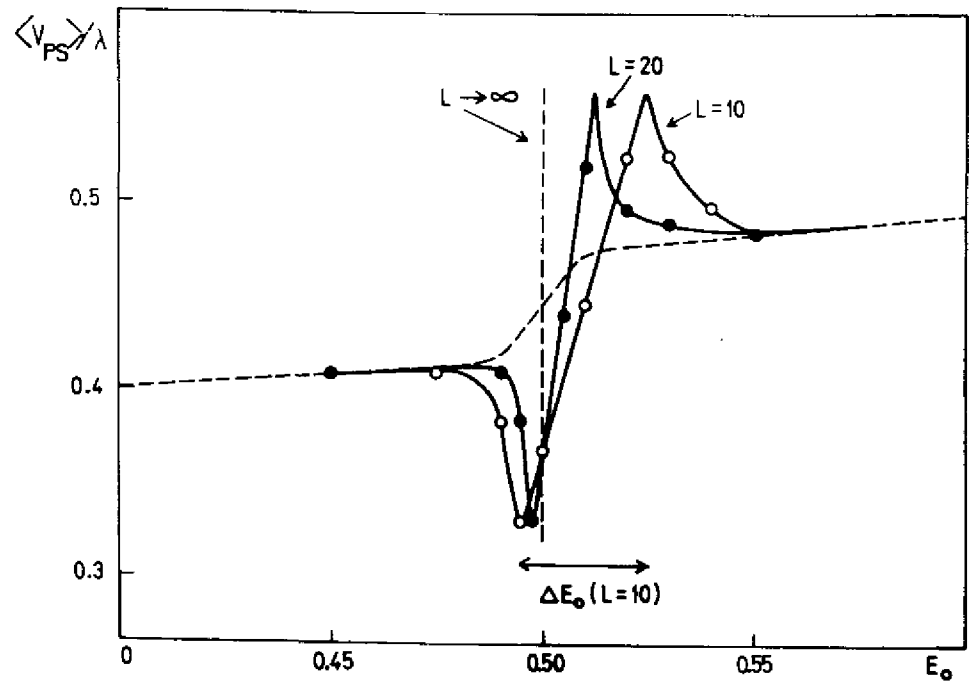
$\langle V_{PS} \rangle / \lambda$
L = 20
L → ∞
L = 10
0.5
0.4
0.3
ΔE_o (L = 10)
0
0.45
0.50
0.55
E_o

Fig. 12